



## OPEN ACCESS

## EDITED BY

Mohammad Khursheed Siddiqi,  
Virginia Commonwealth University,  
United States

## REVIEWED BY

Parvez Alam,  
National Institute of Allergy and Infectious  
Diseases (NIH), United States  
Nida Zaidi,  
Indian Council of Medical Research (ICMR),  
India

## \*CORRESPONDENCE

Sumit K. Chaturvedi,  
✉ sumitprof@gmail.com,  
✉ schaturvedi@biophysics.du.ac.in

RECEIVED 31 October 2025

REVISED 19 November 2025

ACCEPTED 26 November 2025

PUBLISHED 08 December 2025

## CITATION

Ruhela K,  
Subham, Maurya SS, Dwivedi-Agnihotri H and  
Chaturvedi SK (2025) In silico study of  
structure-based screening of inhibitors to block  
PrP<sup>C</sup> conversion and amyloid aggregation.  
*Front. Chem. Biol.* 4:1736396.  
doi: 10.3389/fchbi.2025.1736396

## COPYRIGHT

© 2025 Ruhela, Subham, Maurya, Dwivedi-Agnihotri and Chaturvedi. This is an open-access article distributed under the terms of the [Creative Commons Attribution License \(CC BY\)](https://creativecommons.org/licenses/by/4.0/). The use, distribution or reproduction in other forums is permitted, provided the original author(s) and the copyright owner(s) are credited and that the original publication in this journal is cited, in accordance with accepted academic practice. No use, distribution or reproduction is permitted which does not comply with these terms.

# In silico study of structure-based screening of inhibitors to block PrP<sup>C</sup> conversion and amyloid aggregation

Kamakshi Ruhela<sup>1</sup>, Subham<sup>1</sup>, Shailendra S. Maurya<sup>2</sup>,  
Hemlata Dwivedi-Agnihotri<sup>1</sup> and Sumit K. Chaturvedi<sup>1\*</sup>

<sup>1</sup>Department of Biophysics, University of Delhi, New Delhi, India, <sup>2</sup>Department of Hematology (SCRC), Chromatin Architecture Laboratory, Sanjay Gandhi Postgraduate Institute of Medical Sciences, Lucknow, India

Prion diseases are a group of progressive and fatal neurodegenerative diseases, caused by the transformation of cellular prion protein (PrP<sup>C</sup>) into a misfolded pathogenic isoform (PrP<sup>Sc</sup>). Several strategies have been proposed to mitigate different stages of prion propagation and aggregation. One such approach involves limiting the availability of PrP<sup>C</sup> substrate for misfolding. Various compounds have been shown to inhibit the conversion process; however, no compounds have been identified that are potentially effective in curing prion diseases. Therefore, identifying novel inhibitors targeting key stages of PrP misfolding is essential. This study aims to identify potential anti-prion compounds through a comparative *in silico* approach, which involves molecular docking, pharmacophore-based modelling, and ADMET analysis, using known inhibitors (such as anle138b, GN8, and resveratrol). Through this approach, we have identified some novel compounds that possess the potential to cure prion diseases. Molecular docking results revealed critical protein-ligand interactions, which were later used to construct pharmacophore models. These models directed virtual screening to find structurally and functionally analogous compounds. Drug-likeness and pharmacokinetic properties were evaluated through ADMET profiling. Furthermore, we also analysed whether these screened compounds could reproduce the key interactions seen in known inhibitors, which led to the identification of three potential anti-prion compounds. It reflects the potential of pharmacophore-based high-throughput virtual screening when discovering structurally diverse compounds with similar target profiles. Further validation through molecular dynamics simulations and experimental assays is necessary to confirm their efficacy and advance therapeutic development against prion diseases.

## KEYWORDS

neurodegenerative disease, protein aggregation, protein misfolding, molecular docking, pharmacophore-based modelling, ADMET analysis

## 1 Introduction

Prion diseases, collectively known as Transmissible Spongiform Encephalopathies (TSEs), are a group of unusual, progressive, and fatal neurodegenerative disorders that primarily affect mammalian species, including humans, sheep, goats, elk, and others. TSEs are mainly caused by altering normal prion protein (PrP<sup>C</sup>) into an abnormal pathogenic

form called (PrP<sup>sc</sup>). The histopathological feature is the accumulation of these pathogenic misfolded/abnormal proteins in the central nervous system, with less frequent deposition in the peripheral nervous system. (Uttley et al., 2020; Prusiner, 2001; Cunha, Nascimento, and Oliveira, 2021; Pan et al., 1993; Prusiner, 1982; McKinley, Bolton, and Prusiner, 1983). Human prion disease includes a distinct group of neurodegenerative disorders such as Creutzfeldt–Jakob disease (CJD), kuru, fatal familial insomnia (FFI), Gerstmann–Sträussler–Scheinker disease (GSS), and variably protease-sensitive prionopathy (VPSPr) (Huang, Chen, and Zhang, 2015; Geschwind, 2015; Collinge, 2001; Asher and Gregori, 2018; Imran and Mahmood, 2011). According to the aetiology, these neuro-disorders are further classified into three different groups: occur as autosomal dominantly inherited conditions, sporadically, and are afflicted with exposure to infectious prions, which includes iatrogenic transmission (Prusiner, 1998; Geschwind, 2015; Jankovska et al., 2021).

In humans, prion diseases include Creutzfeldt–Jakob disease (CJD) and its various variants (such as sporadic, familial, iatrogenic, and variant CJD), Gerstmann–Sträussler–Scheinker syndrome (GSS), fatal familial insomnia (FFI), and Kuru, which have historical significance (Asher and Gregori, 2018; Manix et al., 2015). These conditions consist of symptoms like dementia, behavioural alteration, insomnia, ataxia, and, in severe cases, can lead to coma and even death (Trevitt and Collinge, 2006; Paterson, Takada, and Geschwind, 2012; Geschwind, 2010). Neurotoxicity involves mitochondrial impairment, synaptic dysfunction, activation of microglial and oxidative stress, which leads to progressive loss of neurons (Plascencia-Villa and Perry, 2023; Qin, Sun, and Li, 2024). Mutations in the PRNP gene are the primary cause of the genetic forms, whereas acquired forms can result from contaminated medical tools, blood transfusions, or the ingestion of prion-infected food (Jankovska et al., 2021; Bagyinszky et al., 2018; Nafe, Arendt, and Hattingen, 2023).

On the other hand, animal prion diseases include scrapie in sheep and goats, bovine spongiform encephalopathy (BSE), also known as mad cow disease, in cattle, and chronic wasting disease (CWD), also referred to as zombie deer disease, in elk, deer, and moose. Most prion diseases exhibit a significant species barrier; however, cross-species transmission has occurred, most notably in the case of BSE, which has led to variant CJD in humans. Prion diseases can arise sporadically without a known cause, genetically due to inherited PRNP mutations, or through exposure to medical procedures, cultural practices, or diet. Prion diseases, such as BSE and variant CJD, highlight their potential effect on both human and animal health, as well as food safety. Continuous worldwide surveillance of animal prion outbreaks is crucial to prevent zoonotic transmission and help in safeguarding the food supply chain (Imran and Mahmood, 2011; Sigurdson and Miller, 2003; Béringue, Vilotte, and Laude, 2008; Sejvar, Schonberger, and Belay, 2008; Institute of Medicine Forum on Emerging Infections, 2002).

Pathologically, prion disease is further categorised into two groups: spongiform encephalopathies and the PrP amyloidosis. The spongiform encephalopathies, such as CJD and most FFI, where the main pathological feature is spongiform change, which affects multiple brain regions, whereas the PrP-amyloidosis, such as Gerstmann–Sträussler–Scheinker disease (GSS) and other genetic

forms, are characterised by the accumulation of PrP deposition in vessel-associated cerebral amyloid angiopathy (CAA) and parenchymal (Tee et al., 2018; Sejvar et al., 2008).

The cellular prion protein (PrP<sup>c</sup>) is a glycosylphosphatidylinositol (GPI)-anchored membrane protein mainly localised in the neuronal cells (Peters et al., 2003; Vey et al., 1996). The cellular PrP<sup>c</sup> is mainly composed of  $\alpha$ -helices. Structurally, the PrP<sup>c</sup> sequence comprises a flexible N-terminal domain facilitating copper ions binding; a hydrophobic core; and a C-terminal globular domain (Surewicz and Apostol, 2011; Maiti and Surewicz, 2001; Riesner, 2003; Zahn et al., 2000). The physiological role of PrP<sup>c</sup> is not well investigated still the literature does elicit its importance in various biological processes such as cellular signalling, neuroprotection, antioxidant defence, and maintenance of synaptic function (Roucou, Gains, and LeBlanc, 2004; Wulf, Senatore, and Aguzzi, 2017; Petit et al., 2013). The mutation in the PRNP gene or exposure to a foreign PrP<sup>sc</sup> molecule causes cellular PrP<sup>c</sup> to be converted into its misfolded,  $\beta$ -sheet-rich, insoluble, and protease-resistant conformer (PrP<sup>sc</sup>), which is thought to be infectious (Bernardi and Bruni, 2019; Prusiner, 1998). The PrP<sup>sc</sup> aggregates very fast and leads to amyloid formation, which is highly neurotoxic. The conversion of PrP<sup>c</sup> into its pathogenic PrP<sup>sc</sup> form is proposed to occur via two mechanisms: (i) a nucleation-dependent polymerisation in which a seed is formed, which recruits and stabilises the aberrant conformation of PrP<sup>sc</sup>, which in normal physiological conditions remains in dynamic equilibrium with PrP<sup>c</sup> and (ii) the template-assisted model, which states that the interaction of exogenous PrP<sup>sc</sup> with endogenous PrP<sup>c</sup> induces the conformational changes in PrP<sup>c</sup> leading to its conversion to PrP<sup>sc</sup>. The native PrP<sup>c</sup> is rich in  $\alpha$ -helical content, which is the primary reason for its being soluble in the biological milieu and rendering it protease-sensitive (Alvarez-Martinez et al., 2011; Viles et al., 2001). PrP<sup>sc</sup>, on the contrary side, contain nearly 43%  $\beta$ -sheet, which shoots up to 54% in the protease-resistant fragments of PrP<sup>sc</sup> (27–30) (Pan et al., 1993). The C-terminal domain of PrP<sup>sc</sup> forms extensive cross- $\beta$  fibril aggregates because this region contains abundant  $\beta$ -sheet structures stabilised by extensive hydrogen bonds between these strands. The insolubility and high aggregation tendency of PrP<sup>sc</sup> are the biggest challenges that have prevented researchers from deciphering the atomic structure of membrane-bound PrP<sup>sc</sup> (Jarrett and Lansbury, 1993; Prusiner, 1998; Wan et al., 2015; Wille and Requena, 2018).

Anti-prion drug discovery primarily focuses on preventing the conversion of native cellular prion (PrP<sup>c</sup>) into pathogenic form (PrP<sup>sc</sup>). Different strategic approaches have been proposed to modulate different stages of prion production and PrP<sup>sc</sup> aggregation formation (Uliassi et al., 2023). One such strategy involves the limiting of substrate availability, which is required for the misfolding of the PrP<sup>c</sup> protein. However, considering the neuroprotective and homeostatic functions of PrP<sup>c</sup>, prolonged depletion may disrupt these functions. Another strategy focuses on stabilising the native  $\alpha$ -helical structure of PrP<sup>c</sup>, thereby preventing its conversion into the toxic  $\beta$ -sheet-rich PrP<sup>sc</sup> form. Similarly, blocking the molecular interaction between partially unfolded PrP<sup>c</sup> and existing PrP<sup>sc</sup> conformers is also a key strategy to prevent the initial nucleation events of misfolding. Moreover, preventing PrP<sup>c</sup> recruitment by PrP<sup>sc</sup> through inhibition of template-directed conversion can halt the growth of

the diseased form. Additional strategies include inhibition of PrP<sup>Sc</sup> polymer formation and aggregation into lethal amyloid fibrils via disruption of  $\beta$ -sheet stacking and intermolecular hydrogen bonding. Lastly, enhancing the autophagy and proteasomal pathways can speed up the clearance of diseased proteins and protect against neurotoxicity. Collectively, these approaches form a comprehensive framework for combating prion diseases by targeting different stages of prion formation and accumulation inside the cell (Uliassi et al., 2023).

Various anti-prion compounds have been investigated, such as chlorpromazine, Pentosan polysulfate, suramin, Anle138b, and anti-malarial molecules like quinacrine, which have been reported as potential inhibitors of prion diseases, targeting various stages of prion propagation and aggregation (Doh-Ura, Iwaki, and Caughey, 2000; Doh-ura et al., 2004; Vallabh et al., 2023; Wagner et al., 2013; Barreca et al., 2018). Similarly, chlorpromazine, a phenothiazine antipsychotic, reallocates PrP<sup>Sc</sup> to late endosomes/lysosomes without modulating the localisation of PrP<sup>C</sup>; however, *in vivo* and clinical outcomes remain modest. Pentosan polysulfate (PPS), a sulfated glycosaminoglycan, likely declines PrP<sup>Sc</sup> levels by disrupting PrP<sup>C</sup>-PrP<sup>Sc</sup> interactions at the cell surface. However, its specific mechanism is unclear and has limited clinical benefits. *In silico* screening techniques are gradually being integrated into therapeutic development to rapidly identify and augment potential drug candidates. Methods like AI-based drug discovery, molecular docking, virtual screening and pharmacophore modelling enable the researchers to screen large compound libraries in one run before *in vitro* experiments hence thereby reducing both time and cost. These approaches have been used in determining inhibitors of Hepatitis B antiviruses, such as a pyrazole moiety iCDM-34, and in repurposing current antivirals, with various AI-guided drug discovery platforms now supporting pre-clinical trials for antiviral and cancer therapy. As such, computational tools continue to advance, and they are accelerating the transition from molecular prediction to modern therapeutic outcomes. (Doh-ura et al., 2004; Tsuboi, Doh-Ura, and Yamada, 2009; Ugbaja et al., 2025; Elmessaoudi-Idrissi et al., 2018). In prion research, a pre-silico study shaped a similar therapeutic exploration. For instance, tricyclic acridines such as quinacrine and phenothiazines like chlorpromazine were among the earliest *in silico* identified drugs that show inhibitory activity against misfolded prion protein. These drugs, already approved for other therapeutic uses, were shown through computational docking and cell-based assays to inhibit aggregation formation in prion-infected N2a cells. Also, the NMR studies and structural modelling demonstrated that quinacrine binds to the globular domain of recombinant human PrP, particularly involving residues Tyr225-Gln227 on helix 3 (region 1). Though quinacrine advanced to clinical trials for Creutzfeldt-Jakob disease (CJD), it shows limited efficacy, emphasising the challenges of translating *in silico* and *in vitro* findings into optimal clinical outcomes. Nonetheless, such computational studies show how *in silico* screening has fast-tracked the identification and structural optimisation of anti-prion compounds and endures to guide rational drug design efforts in disease areas (Thompson et al., 2011).

High-throughput virtual screening and structure-based drug design are cost-effective strategies that accelerate drug discovery. Novel aggregation inhibitors, such as the diphenyl pyrazole

derivative Anle138b, efficiently prevent the PrP<sup>Sc</sup> oligomerisation formation, demonstrating high blood-brain barrier penetration, CNS bioavailability, and minimal adverse effect (Wagner et al., 2013; Leidel et al., 2011). Compounds such as GN8 (3-Benzyl-5-[(2-hydroxy-3-nitrophenyl) methyl]-2-sulfanylidene-1,3-thiazolidin-4-one) and its carbazole derivative 2b stabilise PrP<sup>C</sup> or inhibit the conversion of PrP<sup>Sc</sup>, with 2b additionally offering therapeutic and diagnostic potential because of its intrinsic fluorescence (Kuwata et al., 2007; Kimura et al., 2013). Natural occurring polyphenolic compounds such as resveratrol inhibit prion fibril formation and protect against cytotoxicity, via an autophagy-mediated mitochondrial mechanism (Jeong et al., 2012). Finally, an FDA-approved drug for migraine, flunarizine, affects ribosome protein folding activity and reduces prion propagation, with structurally related compounds showing similar anti-prion and anti-aggregation effects (Wermuth CG. 2004; Wermuth C. G. 2004). In our study, we performed *in silico* virtual screening assisted by molecular docking against the human prion protein and its fibrillar form. This study aims to identify novel anti-prion compounds through a comparative study, followed by pharmacophore-based modelling and ADMET analysis, with known inhibitors, through which we determined the potential novel compound. We also analysed the screened compounds' reproducibility key interactions of known inhibitors at the residual level, which revealed three potential anti-prion compounds. Despite extensive research, no effective therapy for prion diseases remains. Therefore, identifying novel inhibitors targeting key stages of PrP misfolding is essential, since the experimental structural elucidation of PrP<sup>Sc</sup> structure remains challenging. In this context, computational study, such as molecular docking and virtual screening, provides a valuable alternative for the rational study of the potential discovery of inhibitors.

## 2 Materials and methods

A set of known prion disease inhibitors was identified from a literature review and selected for docking against the human prion protein (PrP<sup>C</sup>), and prion fibril structures are listed in Table 1. PyRx was used for all computational analyses using an integrated software with AutoDock Vina as the docking tool.

### 2.1 Receptor preparation

The 3D structures of the prion protein and prion fibril were retrieved from the Protein Data Bank (PDB) in.pdb format. Two demonstrative PDB entries were used, i.e., 1QLZ (PrP<sup>C</sup>) and 6LNI (fibrillar aggregates). UCSF ChimeraX were used for receptor preparation, where all non-essential molecules, including ions, water molecules, ligands, and heteroatoms, were removed to minimise the interference with docking. Polar hydrogen molecules were added, and the Kollman charges were assigned to parametrise the force field on the receptor molecule. The structure of receptors was further subjected to minimisation of energy to reduce steric hindrance and geometry optimisation. The prepared structures were saved in.pdb format and then changed to.pdbqt within PyRx for a docking study (Meng et al., 2011).

TABLE 1 Docking analysis of known inhibitors with 1QLZ (Human prion protein) and 6LNI (Amyloid fibril).

Receptor	Ligands (PubChem CID)	Binding affinity (kcal/mol)
1QLZ (human prion protein)	Quinacrine (237)	-4.7
	Chlorpromazine (2726)	-5.6
	Pentosan polysulfate (37720)	-6.2
	Anle138b (44608289)	-6.7
	GN8 (16122598)	-6.5
	Resveratrol (445154)	-5.5
6LNI (amyloid fibril)	Quinacrine (237)	-5.3
	Chlorpromazine (2726)	-5.5
	Pentosan polysulfate (37720)	-5.5
	Anle138b (44608289)	-10
	GN8 (16122598)	-6.5
	Resveratrol (445154)	-7.7

## 2.2 Preparation of ligands

Ligands were extracted from the databases ZINC15 and PubChem in.sdf format. These were imported into PyRx and then converted to.pdbqt format using the built-in Open Babel tool. Before performing docking, geometry optimisation, and energy minimisation were done with the Universal Force Field (UFF) to obtain the lowest-energy conformations. Torsional flexibility of the selected ligands was automatically determined during.pdbqt conversion.

## 2.3 Molecular docking

Simulations of docking were performed using AutoDock Vina within PyRx. Both 6LNI and 1QLZ receptors were changed into.pdbqt format, and grid box parameters were outlined to enable blind docking of the complete protein. For 1QLZ (PrP<sup>c</sup>): Grid size parameter (Å): X: 49.63, Y: 36.29, Z: 34.45; center: X: -3.92, Y: 1.37, Z: 0.44. For 6LNI (fibrils): Grid size parameter (Å): X: 135.39, Y: 110.14, Z: 30.77; centre: X: 202.92, Y: 202.92, Z: 230.90. AutoDock Vina uses a Lamarckian Genetic Algorithm, which proficiently analyses the conformational space and uses a hybrid empirical scoring function for ranking different binding poses. The output contained the docked poses with predicted binding affinities in kcal/mol (Meng et al., 2011; Rizvi et al., 2013).

## 2.4 Visualisation and interaction study

UCSF ChimeraX and PyMOL 3.1 were used to evaluate the correct ligand orientation within the binding pocket for visualisation and interaction studies of docking results. The top-ranked ligand-receptor complexes were further scrutinised in BIOVIA Discovery Studio Visualizer, where comprehensive interaction profiling was performed, including different bonding types such as hydrogen bonding, electrostatic interactions,  $\pi$ - $\pi$  stacking, Salt bridges, and

hydrophobic interactions. Two-dimensional interaction maps and three-dimensional binding site visualisations were created to simplify the interpretation of docking results.

## 2.5 Pharmacophore modelling

A ligand-based pharmacophore model (LBPM) was computed from the best-performing inhibitors to capture interaction-relevant features, which are essential for the electrostatic interactions of the prion protein or fibril. Using Pharmit, two complementary approaches were carried out: Pharmacophore modelling, i.e., Shape-constrained pharmacophore modelling, where the ligand shape was defined as inclusive. In contrast, the shape of the receptor binding pocket was set as exclusive. This allowed prioritization of compounds with both correct pharmacophoric characteristics and optimal spatial fitting. While in Pharmacophore modelling without shape constraints, an unconstrained model was created to explore a broader chemical space and capture the active compounds with pharmacophoric similarity, despite their steric complementarity difference (Giordano et al., 2022; Sunseri and Koes, 2016).

## 2.6 Virtual screening

In this study, a set of known inhibitors was primarily identified through an extensive literature review on the basis of their experimentally validated anti-prion activity, availability of structural data for *in silico* study, and compliance with well-known drug likeness criteria. Furthermore, these inhibitory compounds were used as reference compounds for identifying novel potential inhibitory compounds. To further explore new drug candidates, the developed pharmacophore models were used to screen chemical libraries from the PubChem and ZINC databases. The selected hits were re-docked against PrP<sup>c</sup> and fibrillar structures to confirm their binding affinities and interaction properties.

## 2.7 ADMET profiling

The selected ligands were further assessed for their pharmacokinetic and toxicity properties using SwissADME, which focuses on Absorption, Distribution, Metabolism, Excretion, and Toxicity (ADMET) parameters. Compounds with optimal bioavailability, low predicted toxicity, and acceptable physicochemical properties were kept for in-depth analysis (Guan et al., 2019).

## 2.8 Docking and interaction analysis of screened compounds

The final set of compounds was then evaluated for molecular docking studies against both PrP<sup>c</sup> and fibril structures. In-depth binding interaction analyses were performed to detect the potential anti-prion inhibitors with high affinity and drug-like properties for contemplation in future *in vitro* validation studies.

# 3 Results

## 3.1 Binding energies

The comparative docking analysis was performed using PyRx, an integrated software with AutoDock Vina as the docking engine. To evaluate the binding affinities of known prion inhibitors against the 1QLZ (human prion protein) and 6LNI (Amyloid Fibril of prion protein).

The set of the same six known Compounds was used for screening against both 1QLZ and 6LNI, which show favourable binding energies ranging from  $-6.2$  to  $-10.0$  kcal/mol, signifying a promising potential interaction with both targets. Among the six tested inhibitors, anle138b (Pubchem CID 16122598) showed the highest binding affinity ( $-6.7$  kcal/mol) towards the 1QLZ (human prion protein). In contrast, Pentosan polysulfate (Pubchem CID 37720) demonstrated the moderate binding affinities ( $-6.2$  kcal/mol) to 1QLZ.

On the other hand, anle138b (Pubchem CID 16122598) exhibited the highest binding affinity ( $-10$  kcal/mol) and resveratrol (Pubchem CID 445154) exhibited the highest binding affinity ( $-10$  kcal/mol) towards the 6LNI (Amyloid Fibril). At the same time, GN8 showed relatively similar binding affinity towards the native form of prion protein and fibrillar forms ( $-6.5$  kcal/mol). This indicates that GN8 binds to the  $\alpha$ - $\beta$ 2 loop (notably residue N159), helix B (residues V189, T192, K194), and the BC loop (E196) in PrP<sup>c</sup>, preventing conformational conversion to PrP<sup>sc</sup> and stabilising efficacy.

In comparison, a compound previously studied for its capacity to stabilise PrP<sup>c</sup> or to block the replication of PrP<sup>sc</sup>, quinacrine (Pubchem CID 237), showed weaker binding towards PrP<sup>c</sup> ( $-4.7$  kcal/mol) and prion fibrils ( $-5.3$  kcal/mol). Similarly, Chlorpromazine (Pubchem CID 2726) had limited binding with both forms of the protein (PrP<sup>c</sup>:  $-5.6$  kcal/mol; fibrils:  $-5.5$  kcal/mol). This concluded that neither the Chlorpromazine nor the quinacrine shows strong binding affinities against the 1QLZ and 6LNI. Their effects are likely due to indirect modulation of protein

trafficking or cellular pathways rather than direct binding, which inhibits the prion protein.

## 3.2 Pharmacophore modelling

Pharmacophore models were constructed from the docking interaction data of anle138b, resveratrol, and GN8 with both the native prion protein and the amyloid fibril (Figures 1, 2). The Pharmacophore model based on Anle138b demonstrated that it incorporated one hydrogen bond acceptor and two hydrophobic interactions, whereas the resveratrol-based model contained two hydrogen bond donors and one hydrophobic interaction. For GN8, the pharmacophore consisted of one hydrogen bond donor, two hydrogen bond acceptors, and two hydrophobic features (Figure 3).

These pharmacophoric features were utilised to construct screening models for discovering novel inhibitors with similar binding characteristics. The virtual screening ensured that the selected compounds exhibited the appropriate drug-like properties. The filters include widely accepted pharmacokinetic parameters: molecular weight between 150 and 500 Da, no more than nine rotatable bonds, logP between 0.7 and 5,  $\leq 5$  hydrogen bond donors,  $\leq 10$  hydrogen bond acceptors, and a polar surface area (PSA) between 20 and 130 Å<sup>2</sup>.

## 3.3 ADMET analysis

For ADMET Analysis (Absorption, Distribution, Metabolism, Excretion, and Toxicity), we use Bioavailability Radar, which is part of the SwissADME platform. SwissADME is an online web tool that is used to evaluate physicochemical properties, drug-like properties, water solubility, pharmacokinetics, lipophilicity, medicinal chemistry, and other molecules. It maps various properties of a molecule, including polarity, total polar surface area, molecular size, lipophilicity, insolubility, instauration, flexibility, GI absorption, BBB permeability, P-gp substrate, and CYP450 Enzyme Inhibition.

From the above ADMET profiling of three resveratrol-derived pharmacophore molecules (PubChem CIDs: 22413641, 69849109, and 155286501) with the amyloid fibril structure (PDB ID: 6LNI), without inclusive ligand and exclusive receptor filters and with these constraints, a set of potential candidates was generated. However, most of these compounds have favourable drug-like properties. Most of the compounds follow the Lipinski's Rule of Five, showing high gastrointestinal (GI) absorption, and were predicted to be permeant to the blood-brain barrier (BBB), which significantly increases the potential as central nervous system (CNS)-active agents. Among the selected compounds, PubChem CID 155286501 displayed the highest binding affinity ( $-8.6$  kcal/mol) to the fibril form of a protein (PDB ID: 6LNI), and also maintained acceptable lipophilicity (LIPO = 2.43) and polarity (63.93 Å<sup>2</sup>). Yet, both 69849109 and 155286501 were foreseen to be P-glycoprotein (P-gp) substrates, which reduce the accumulation of misfolded protein in the brain because of efflux transport. On the other hand, compound 22413641 displays lower binding affinity ( $-5.6$  kcal/mol) and is not a P-gp substrate, which may allow more stable CNS bioavailability.

**(A)**

Pharmacophore Results				Pharmacophore Results			
Name	RMSD	Mass	Rbinds	Name	RMSD	Mass	Rbinds
PubChem-124425731	0.131	313	6	PubChem-124425731	0.131	313	6
PubChem-87450301	0.132	409	7	PubChem-81158051	0.141	281	6
PubChem-81158051	0.141	281	6	PubChem-81162642	0.148	292	3
PubChem-124699033	0.146	337	6	PubChem-89304156	0.150	339	4
PubChem-81626642	0.148	292	3	PubChem-121982904	0.155	291	7
PubChem-89304156	0.150	339	4	PubChem-80305718	0.162	296	8
PubChem-121982904	0.155	291	7	PubChem-124425729	0.163	313	6
PubChem-80305718	0.162	296	8	PubChem-65809876	0.166	279	9
PubChem-124425729	0.163	313	6	PubChem-135748085	0.172	299	5
PubChem-65809876	0.166	279	9	PubChem-64222879	0.174	251	5
PubChem-104315652	0.171	297	7	PubChem-135748083	0.184	343	5
PubChem-135748085	0.172	299	5	PubChem-135748084	0.184	357	6
PubChem-64222879	0.174	251	5	PubChem-121843444	0.184	289	6
PubChem-108794520	0.180	320	7	PubChem-135748063	0.185	333	5
PubChem-108794616	0.180	334	8	PubChem-120236817	0.185	288	7
PubChem-121982629	0.180	279	7	PubChem-108794583	0.185	304	7
PubChem-120693454	0.182	315	7	PubChem-135748083	0.188	343	5
PubChem-124664636	0.184	343	6	PubChem-135748064	0.189	347	6
PubChem-135748083	0.184	343	5	PubChem-108794588	0.190	306	6
PubChem-135748084	0.184	357	6	PubChem-135748074	0.191	306	6
PubChem-121843444	0.184	289	6	PubChem-135748067	0.192	292	5

**(B)**

Pharmacophore Results				Pharmacophore Results			
Name	RMSD	Mass	Rbinds	Name	RMSD	Mass	Rbinds
PubChem-11476298	0.008	444	7	PubChem-90694423	0.004	274	8
PubChem-107113207	0.009	280	5	PubChem-91465498	0.005	296	8
PubChem-51692994	0.012	442	3	PubChem-22413641	0.008	309	6
PubChem-155286501	0.013	309	3	PubChem-163621291	0.008	482	9
PubChem-134130933	0.013	325	7	PubChem-69849109	0.008	357	2
PubChem-15692309	0.013	280	5	PubChem-78830403	0.008	337	8
PubChem-7108916	0.013	376	9	PubChem-11476298	0.008	444	7
PubChem-143572705	0.013	290	3	PubChem-91152516	0.009	257	6
PubChem-4395652	0.015	407	8	PubChem-123442295	0.009	307	5
PubChem-123411233	0.016	304	7	PubChem-107113207	0.009	280	5
PubChem-79528285	0.016	279	3	PubChem-107113207	0.009	280	5
PubChem-74237680	0.016	295	3	PubChem-107113207	0.009	280	5
PubChem-46983504	0.017	304	8	PubChem-54524610	0.009	387	8
PubChem-87648724	0.017	448	5	PubChem-133775822	0.010	342	8
PubChem-140618042	0.018	364	3	PubChem-133566675	0.010	472	5
PubChem-58618059	0.018	287	9	PubChem-95285504	0.010	342	9
PubChem-9867602	0.019	435	4	PubChem-161502466	0.010	436	9
PubChem-91898119	0.019	381	5	PubChem-67166700	0.010	336	4
PubChem-91898119	0.019	381	5	PubChem-90808459	0.010	366	4
PubChem-91898119	0.019	381	5	PubChem-149352474	0.010	398	5
PubChem-91898119	0.019	381	5	PubChem-84172944	0.011	252	3

**(C)**

Pharmacophore Results				Pharmacophore Results				Pharmacophore Results			
Name	RMSD	Mass	Rbinds	Name	RMSD	Mass	Rbinds	Name	RMSD	Mass	Rbinds
PubChem-10972555	0.003	387	9	PubChem-3556914	0.009	468	2	PubChem-133480707	0.022	302	2
PubChem-67223225	0.004	359	4	PubChem-155072877	0.012	322	6	PubChem-122355901	0.025	330	6
PubChem-110315076	0.006	382	2	PubChem-135204690	0.014	446	7	PubChem-141769046	0.025	206	2
PubChem-156331216	0.006	440	5	PubChem-146442511	0.017	379	6	PubChem-137480575	0.025	302	6
PubChem-135887416	0.007	491	9	PubChem-79562416	0.017	304	6	PubChem-140323505	0.029	263	4
PubChem-97444420	0.007	378	6	PubChem-10524810	0.020	397	8	PubChem-22552389	0.031	474	5
PubChem-8729432	0.007	321	6	PubChem-56502194	0.022	437	9	PubChem-4607555	0.032	384	6
PubChem-114451233	0.007	298	6	PubChem-133480707	0.022	302	2	PubChem-140480586	0.034	293	5
PubChem-160093611	0.008	477	8	PubChem-584323283	0.022	324	4	PubChem-22516430	0.034	382	6
PubChem-146147763	0.008	358	7	PubChem-139357355	0.022	365	1	PubChem-16799235	0.034	358	5
PubChem-135691834	0.008	319	4	PubChem-154042035	0.023	485	5	PubChem-18094552	0.036	364	5
PubChem-75453636	0.008	339	4	PubChem-75450738	0.023	344	5	PubChem-71227320	0.038	335	0
PubChem-97436242	0.008	376	4	PubChem-98652794	0.024	407	3	PubChem-16332825	0.038	374	1
PubChem-113093267	0.008	378	7	PubChem-1714073	0.024	239	2	PubChem-60129776	0.038	360	4
PubChem-71254306	0.008	436	6	PubChem-2866251	0.024	337	7	PubChem-154858299	0.039	480	8
PubChem-163199102	0.008	310	1	PubChem-7710801	0.024	461	2	PubChem-104793672	0.039	265	4
PubChem-144006054	0.008	335	2	PubChem-6724231	0.025	483	7	PubChem-145689901	0.039	335	5
PubChem-4380823	0.008	323	8	PubChem-18823192	0.025	351	8	PubChem-7795368	0.040	410	8
PubChem-13567129	0.008	333	6	PubChem-137118926	0.025	484	4	PubChem-67087664	0.041	364	9
PubChem-140331255	0.008	378	3	PubChem-9006217	0.025	333	6	PubChem-115157516	0.041	261	5
PubChem-140331255	0.008	378	3								
PubChem-133087594	0.008	346	3								
PubChem-8823588	0.008	402	9								

FIGURE 1 Pharmacophore-based virtual screening results (A) for resveratrol in complex with fibril structure (PDB ID: 6LNI), (B) for GN8 in complex with prion protein structure (PDB ID: 1QLZ), and (C) for anle138b with fibril structure (PDB ID: 6LNI).

**(A)**

**(B)**

**(C)**

FIGURE 2 Pharmacophore construction and virtual screening model derived from (A) Anle138b docking insights, (B) resveratrol docking insights and (C) GN8 docking insights.

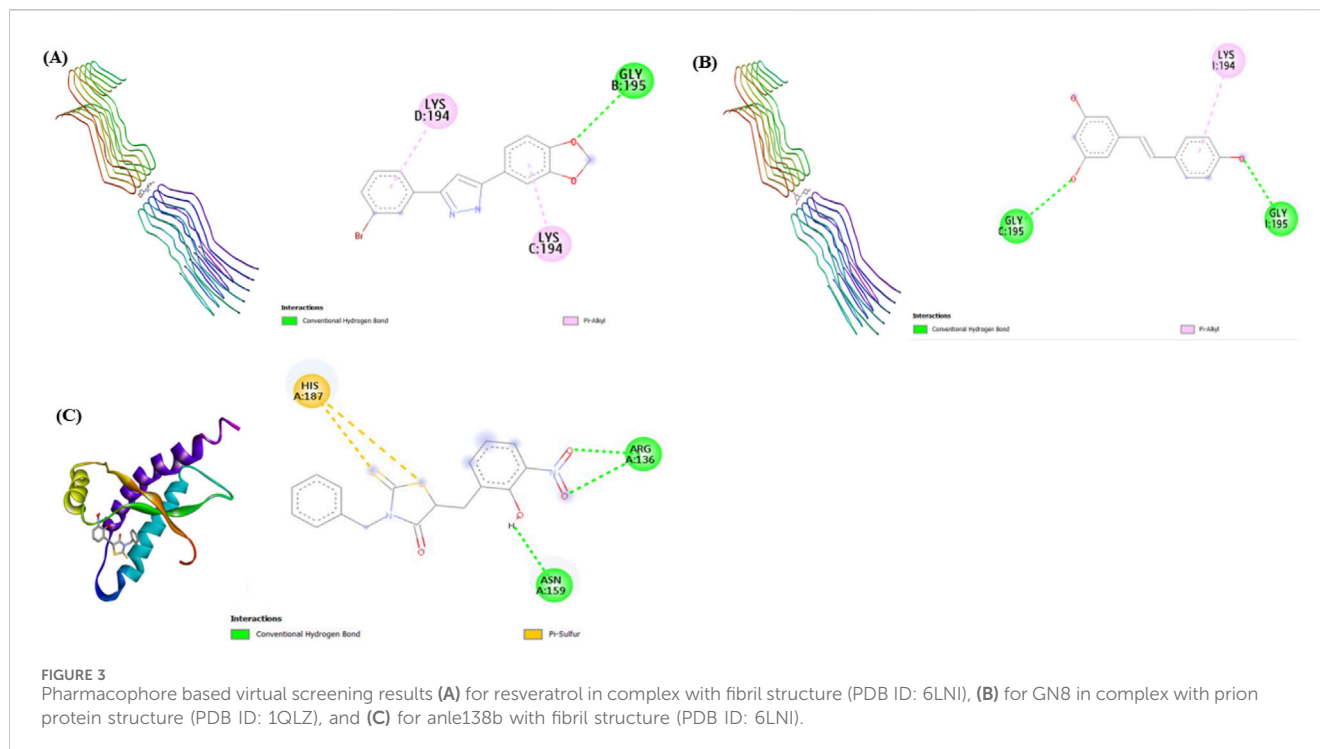


**TABLE 2** ADMET properties and physicochemical properties of Resveratrol-Derived Pharmacophore Compounds targeting Prion fibrils (6LNI).

PubChem ID	ADMET properties		
	22413641	69849109	155286501
Lipophilicity	3.19	2.27	2.43
SIZE (g/mol)	309.42	357.44	309.44
Polarity ( $\text{\AA}^2$ )	43.70	73.16	63.93
Insolubility	-3.57	-3.53	-3.09
Instauration	0.67	0.71	1.00
Flexibility	6	2	3
GI absorption	High	High	High
BBB permeant	Yes	Yes	Yes
Lipinski's rule	Yes	Yes	Yes
P-gp substrate	No	Yes	Yes
CYP450 inhibitor	No	No	No
Binding affinity (kcal/mol)	-5.6	-6.7	-8.6

Inclusively, all three compounds show drug-like properties, but compound 155286501 is considered the most promising candidate because of its stronger binding affinity and physicochemical properties, even though it has potential limitations associated with P-gp-mediated efflux (Table 2).

From the above ADMET profiling of five GN8-Derived Pharmacophore Compounds Identified via Pharmacophore-Based Virtual Screening Against Human Prion Protein. Most of these compounds have favourable drug-like properties. Most of the

compounds follow Lipinski's Rule of Five, showing high gastrointestinal (GI) absorption and being permeable to the blood-brain barrier (BBB), which significantly increases the potential as CNS agents. Among the selected compounds, PubChem CID 80305718 displayed the strongest binding affinity ( $-8.6$  kcal/mol) to the fibril form of a protein (PDB ID: 6LNI), and also maintained acceptable lipophilicity (LIPO = 2.13) and polarity ( $78.43 \text{ \AA}^2$ ). Insolubility values show diversity from  $-2.70$  to  $-3.41$ , whereas unsaturation and flexibility scores specified moderate structural diversity (INSATU: 0.43–0.62; FLEX: 3–9 rotatable bonds). Yet, neither 81626641 nor 121982904 was foreseen to be a P-glycoprotein (P-gp) substrate, which suggests a lesser risk of P-gp efflux and metabolic interference. On the other hand, compound 65809876 displays the weakest binding affinity ( $-5.1$  kcal/mol), which indicates that it might not bind as efficiently to the target protein of interest, while it is pharmacologically promising (Table 3).

Five potential compounds identified via Anle138b pharmacophore screening against prion fibrils (PDB ID: 6LNI) show drug-like properties. All the hits showed high gastrointestinal absorption, Lipinski acquiescence, BBB permeability, and no predicted P-gp substrate or CYP450 inhibition liabilities. Docking studies revealed binding affinities ranging from  $-5.4$  to  $-10.3$  kcal/mol, with PubChem CID 133480707 displaying the strongest interaction ( $-10.3$  kcal/mol) and PubChem CID 141769046, 79562416 and 67221925 showing moderate affinity  $-7.7$ ,  $-7.8$  and  $-6.9$  kcal/mol, respectively, with prion fibrils. Overall, these results highlight the shortlisted molecules as promising CNS-penetrant scaffolds for further optimisation. At the same time, non-BBB-permeable compounds were excluded from further consideration due to limited potential in targeting prion pathologies (Table 4).

TABLE 3 ADMET and Physicochemical Properties of GN8-Derived Pharmacophore Compounds targeting Human Prion Protein (1QLZ).

ADMET properties					
PubChem ID	81158051	81626641	121982904	80305718	65809876
Lipophilicity	2.04	2.83	2.83	2.13	2.39
SIZE (g/mol)	281.28	292.37	291.34	296.34	279.33
Polarity (Å <sup>2</sup> )	75.63	73.40	75.63	78.43	75.63
Insolubility	-2.70	-3.41	-3.18	-2.94	-2.71
Instauration	0.43	0.62	0.50	0.47	0.47
Flexibility	6	3	7	8	9
GI absorption	High	High	High	High	High
BBB permeant	Yes	Yes	Yes	Yes	Yes
Lipinski's rule	Yes	Yes	Yes	Yes	Yes
P-gp substrate	No	No	No	No	No
CYP450 inhibitor	No	No	No	No	No
Binding affinity (kcal/mol)	-5.9	-5.8	-5.8	-6.0	-5.1

TABLE 4 ADMET Properties and Physicochemical Properties of Anle138b derived Compounds targeting Fibrils of Prion (6LNI).

ADMET properties					
PubChem CID	133480707	141769046	137480575	79562416	67221925
Lipophilicity	2.41	3.67	2.02	1.58	1.78
SIZE (g/mol)	302.28	206.32	302.37	303.80	359.33
Polarity (Å <sup>2</sup> )	59.21	20.23	58.64	71.62	72.62
Insolubility	-3.60	-3.30	-2.79	-2.56	-3.35
Instauration	0.29	0.71	0.41	0.46	0.29
Flexibility	2	2	6	6	4
GI absorption	High	High	High	High	High
BBB permeant	Yes	Yes	Yes	Yes	Yes
Lipinski's rule	Yes	Yes	Yes	Yes	Yes
P-gp substrate	No	No	No	No	No
CYP450 inhibitor	No	No	No	No	No
Binding affinity (kcal/mol)	-10.3	-7.7	-5.4	-7.8	-6.9

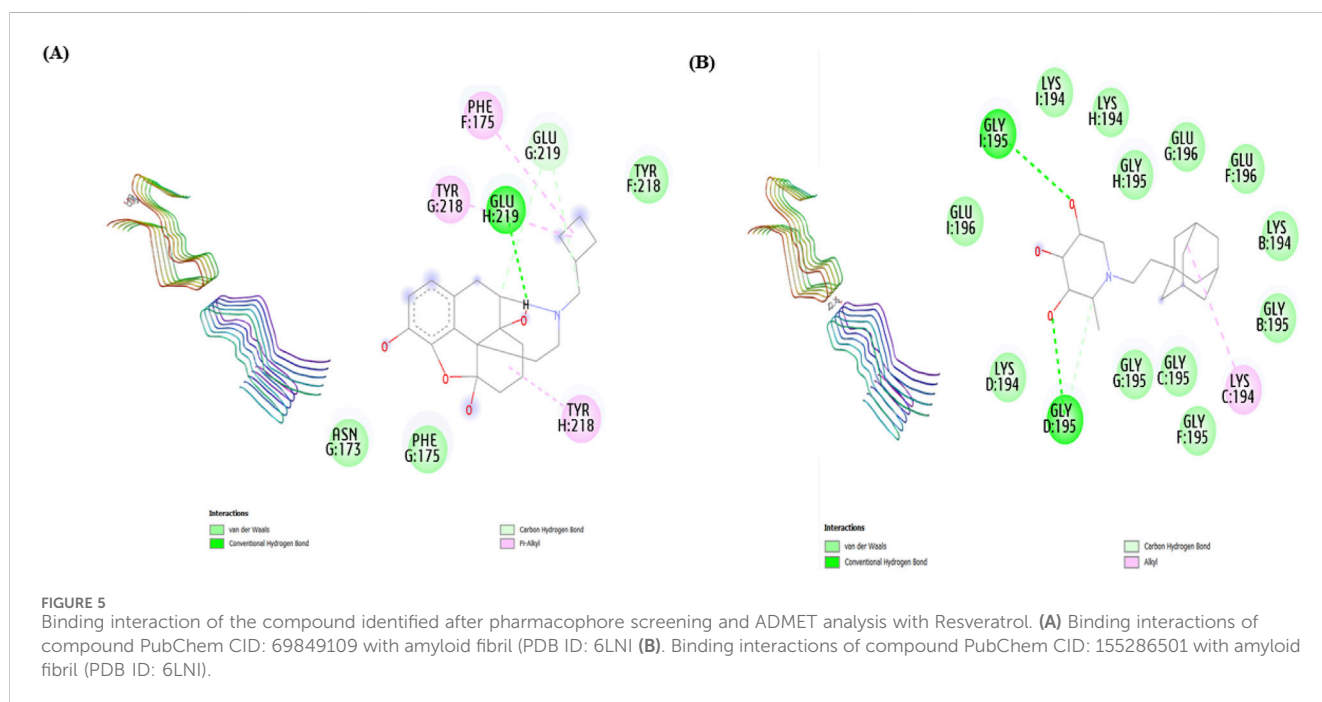
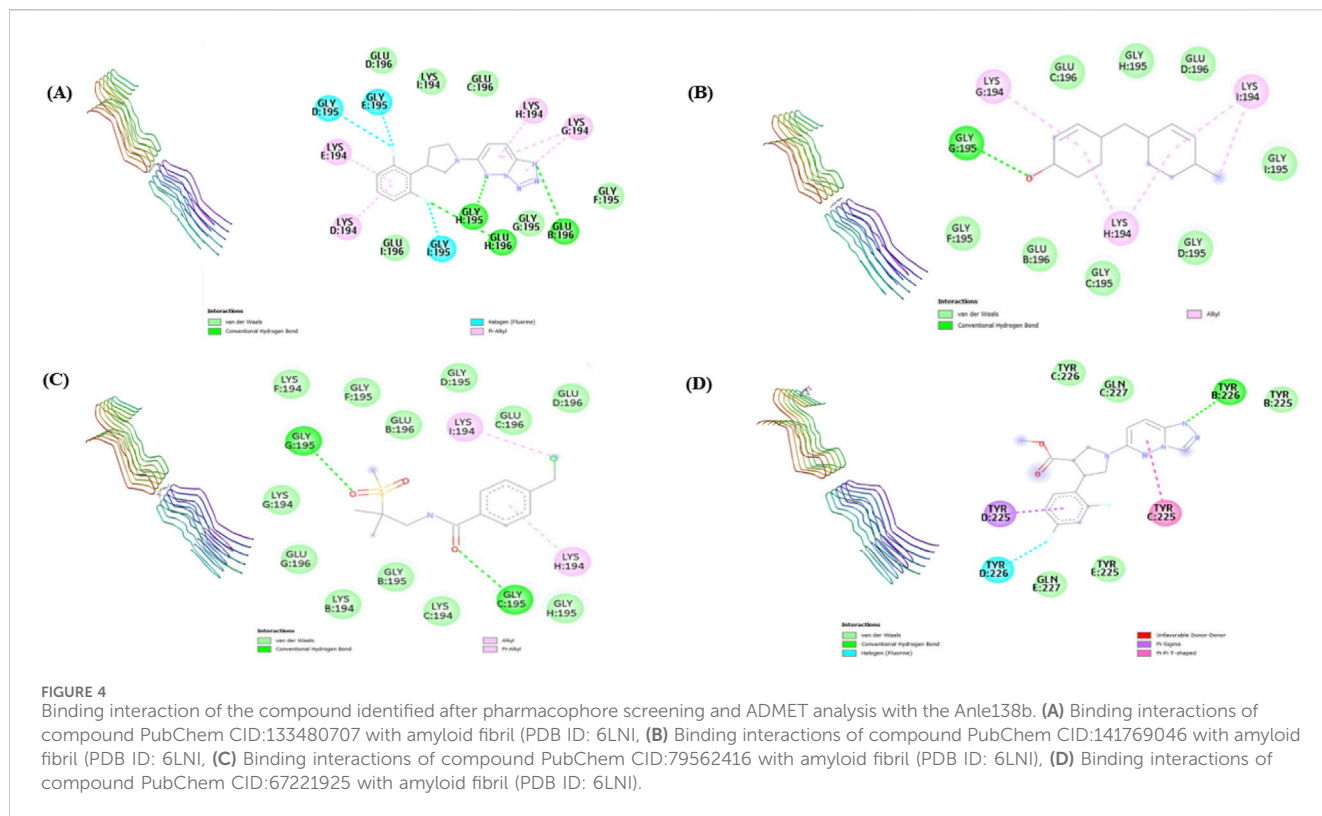
### 3.4 Binding interactions

For anle138b docking binding interactions to the amyloid fibril (PDB ID: 6LNI). The key residues in the site involved a hydrogen bond at GLY B:195, LYS D:194 and LYS C:194, which show a hydrophobic interaction. Among the pharmacophore-derived hits, only a few recapitulated these interactions, such as PubChem CID 133480707, which maintained a hydrophobic interaction with LYS C:194 (Figure 4). Whereas for resveratrol, the key interacting residues were included by a hydrogen bond with GLY C:195 and GLY I:195 and a hydrophobic interaction with LYS I:194. However,

none of the pharmacophore hits of resveratrol reproduce these specific interactions (Figure 5).

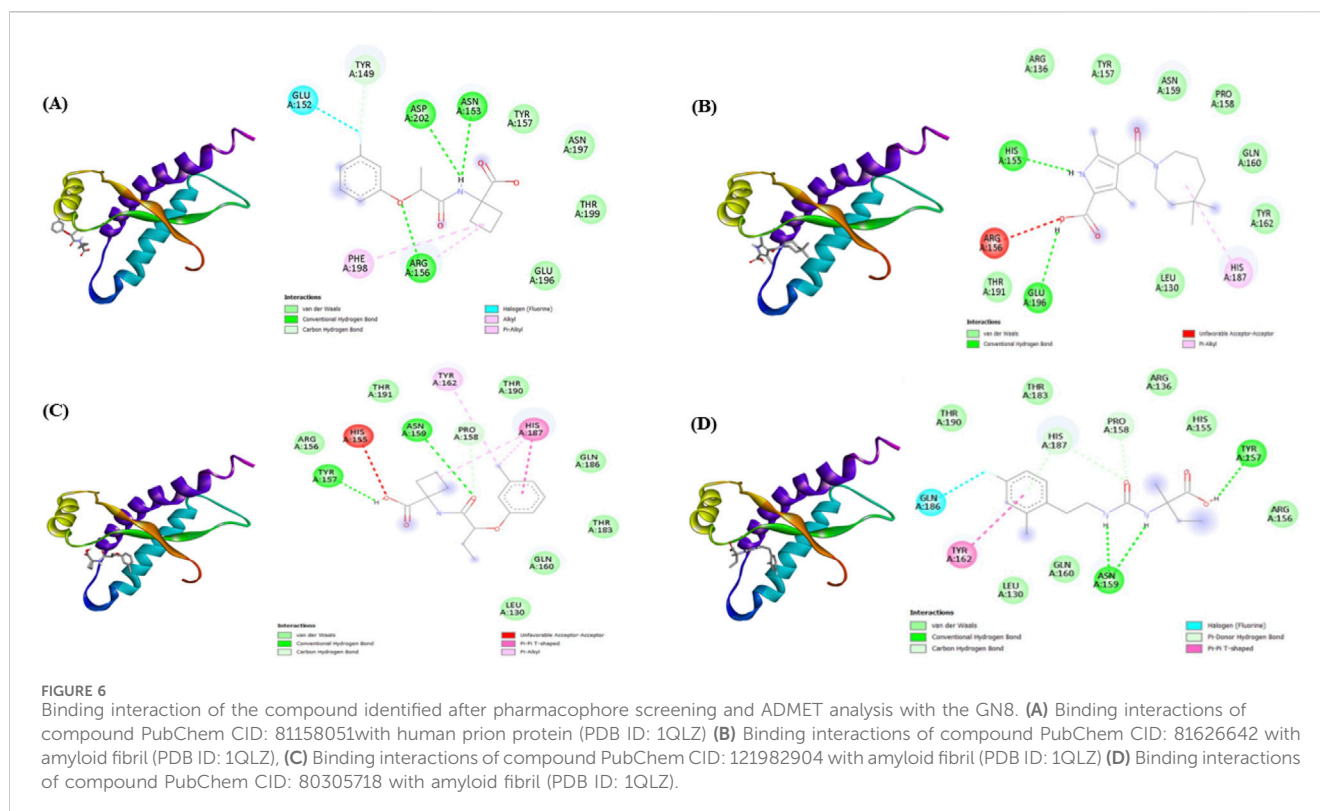
In the case of GN8 and the prion protein (PDB ID: 1QLZ) interaction, the key residues were ARG A:136 and ASN A:159 (hydrogen bond), and HIS A:187 (hydrophobic interaction). Some pharmacophore hits possess similar binding, like PubChem CID 121982904 and CID 80305718, which show identical interactions with amino acid ASN A:159 (Figure 6).

It is noteworthy that only some hits show similar residue-level interactions with known inhibitors; however, this does not necessarily imply a lack of inhibitory activity for these



compounds, since pharmacophore-based virtual screening emphasises preserving main functional similarity rather than reproducing precise intermolecular contacts. Further validation, like interaction fingerprinting or experimental evaluation, is required to confirm the potential therapeutic relevance of these identified compounds.

Due to the autocatalytic secondary nucleation nature of PrP<sup>Sc</sup>, through which aggregates proliferate, our approach should focus on identifying the compounds that can bind at catalytic surface sites of the aggregates, so they can potentially interfere with further growth and aggregation accumulation.



## 4 Discussion

In this study, comparative molecular docking and pharmacophore modelling-based virtual screening of novel compounds have been studied using known compounds against both the native human prion protein and its amyloid fibrillar form. The primary objective is to elucidate the mechanism of prion aggregation and identify novel candidates with potential therapeutic activity against modulating this process by analysing how this compound interacts with the native and aggregated forms of protein, through assessment of binding energy, binding affinities, and ADMET properties.

Compounds listed in Table 1 as already known anti-prion compounds, it was found that resveratrol and Anle138b how the highest binding affinities ( $-10.0$  and  $-7.7$  kcal/mol, respectively) towards the 6LNI (Amyloid Fibril). The results align with the prior data that Anle138b exerts its inhibitory effects by binding to pathological aggregates of  $\alpha$ -synuclein and PrP<sup>sc</sup> in a structure-dependent manner, thereby disrupting oligomer formation (Matthes et al., 2017; Wagner et al., 2013). Notably, research indicates that anle138b exhibits no detectable toxicity, demonstrates high blood-brain barrier penetration and possesses significant oral bioavailability. While resveratrol specifically binds to prion protein residues 127–147, the interaction is primarily stabilised by  $\pi$ - $\pi$  interactions and additionally by hydrogen bonds (Li et al., 2017). Whereas quinacrine and chlorpromazine exhibited weaker affinities ( $-4.7$  to  $-5.6$  kcal/mol), they showed limited efficacy in clinical trials and *in vivo* studies. This reveals that these are less efficient in disrupting pre-existing aggregated PrP fibrils and PrP<sup>sc</sup>. Pentose polyphosphate displayed moderate binding. Studies suggest that

PrP<sup>sc</sup> levels are quickly decreased by pentose polyphosphate without changing the intracellular distribution of PrP<sup>sc</sup>, indicating that it interferes with PrP<sup>sc</sup> replication. Notably, it doesn't affect the location of normal prion protein (PrP<sup>c</sup>). The exact mechanism is unknown, but it most likely involves competitively blocking PrP<sup>c</sup> and PrP<sup>sc</sup> binding through endogenous GAG or PrP<sup>sc</sup> is fragmented at the cell surface by pentose polyphosphate (Yamasaki et al., 2014). Its mechanism shows that it involves PrP<sup>sc</sup> reduction level without modulating the distribution of protein intracellularly. This data, along with computational modelling, suggests that it might interfere with the replication of PrP<sup>sc</sup> rather than directly binding to the protein. GN8 demonstrated similar affinities for both the forms ( $-6.5$  kcal/mol), which revealed that it stabilises the native prion protein (PrP<sup>c</sup>) and prevents its conformational conversion to its pathological isoform, PrP<sup>sc</sup>. Computer simulations and heteronuclear NMR revealed that the area from the B-C loop (E196) to helix B (V189, T192, and K194) and the A-S2 loop (N159) is the particular binding site. This suggests that intercalation of these remote regions (hotspots) impedes the pathogenic conversion process (Kuwata et al., 2002; Uliassi et al., 2023).

Pharmacophore models derived from these compounds (anle138b, resveratrol, and GN8) captured their key interaction features; virtual screening generated numerous hits with favourable physicochemical and CNS bioavailability properties. Among them, PubChem CIDs 133480707 ( $-10.3$  kcal/mol), 69849109 ( $-6.7$  kcal/mol), and 121982904 ( $-5.8$  kcal/mol) comparatively show the highest binding affinities to the reference compounds, respectively, highlighting their potential as optimised analogues, as shown in Table 5.

TABLE 5 List of potential inhibitory compounds of GN8 derived against amyloid fibril (PDB 6LNI) with their amino acid involved and binding affinity.

PubChem CID	Ligand	Amino acids	Interactions	Binding affinity (kcal/mol)
133480707	6-[3-(2,6-Difluorophenyl) pyrrolidin-1-yl] tetrazolo [1,5-b] pyridazine	GLY D:195, GLY C:196, GLY I:195 GLY C: 195 LYS I:194, LYS H:194, LYS B:194, LYS C: 194 GLU D:196, GLY H:195 GLU G:196, GLU F:196, GLY B:195, GLY A: 195, GLU H:196, LYS D:194	Halogen (fluorine), Conventional hydrogen bond, Pi-alkyl, Carbon hydrogen bond, van-der waals	-10.3
141769046	4-[(4-Methylcyclohex-2-en-1-yl) methyl] cyclohex-2-en-1-ol	GLY G:195 LYS G:194, LYS H:194, LYS I:194 GLU C:196, GLY H:195, GLU D:196, GLY I: 195, GLY D:195, GLY C:195, GLU B:196, GLY F:195	Conventional hydrogen bond, Alkyl, Van-der waals	-7.7
79562416	4-(chloromethyl)-N-(2-methyl-2-methylsulfonylpropyl) benzamide (AKOS018118415)	GLY G:195, GLY C:195 LYS I:194, LYS H:194 LYS F:194, GLY F:195, GLU B:196, GLY D: 195, GLU C:196, GLU D:196, GLY H:195, LYS C:194, GLY B:195, LYS B:194, GLU G: 194, LYS G:194	Conventional hydrogen bond, Alkyl, pi-alkyl Van-der waals	-7.8
67221925	Methyl (3S,4S)-4-(2,4-difluorophenyl)-1-[(1,2,4] triazolo [4,3-b] pyridazin-6-yl) pyrrolidine-3-carboxylate (SCHEMBL1946769)	TYR C:226 TYR A:226 TYR C:225 TYR B:225 GLN A:227, TYR A:225, GLN B:227, TYR B:226, GLN C:227, GLN D:227, TYR D:225	Halogen (fluorine), Conventional hydrogen bond, Pi-Sigma, Pi-Pi T shaped, Van-der waals	-6.9

TABLE 6 List of potential inhibitory compounds of Resveratrol derived against the amyloid fibril (PDB 6LNI) with their amino acid involved and binding affinity.

PubChem CID	Ligand	Amino acids	Interactions	Binding affinity (kcal/mol)
69849109	(4R,7aR,12bR)-3-(cyclobutylmethyl)-2,4,5,6,7,13-hexahydro-1H-4,12-methanobenzofuro [3,2-e] isoquinoline-4a,7a,9-triol (SCHEMBL6641239)	PHE F:175, TYR G:218, GLU H:219, GLU G: 219, TYR F:218, ASN G:173, PHE G:175, TYR H:218	Pi-Pi T-shaped, pi-alkyl, Van-der waals	-6.7
155286501	(2R,3R,4R,5S)-1-[2-(1-adamantyl) ethyl]-2-methylpiperidine-3,4,5-triol (SCHEMBL22657524)	GLY I:195, GLY H:195, LYS D:194, LYS B:194, LYS C:194, LYS H:194, GLY D:195, GLY G:195, GLU F:196, GLU G:196, GLY C:195, GLY G: 195, LYS I:194, GLY F:195, GLU I:196, GLY B:195	Conventional hydrogen bond, alkyl, Van-der waals	-8.6

ADMET profiling confirmed that the majority of the hits followed the selection parameters of pharmacokinetics, which include properties such as polarity, total polar surface area, molecular size, lipophilicity, insolubility, instauration, flexibility, GI absorption, BBB permeability, P-gp substrate, and CYP450 Enzyme Inhibition. Among these compounds, PubChem CID 69849109 (-6.7 kcal/mol) of resveratrol-derived compounds fulfils all the parameters, except that it is not a P-glycoprotein (P-gp) substrate, which may affect their CNS bioavailability, as shown in Table 6. Meanwhile, the remaining two compounds favour CNS bioavailability. Yet, compounds found as P-gp substrates or those with high unsaturation may further require chemical optimisation to improve stability and brain preservation.

Residual level analysis revealed that several screened compounds reproduced key interactions of known inhibitors. For anle138b,

Table 7 shows the key residues in the site involved in a hydrogen bond at GLY B:195, LYS D:194, and LYS C:194, which exhibit a hydrophobic interaction; only the compound 133480707 maintained a hydrophobic interaction with LYS C: 194. Meanwhile, for resveratrol, none of the pharmacophore hits reproduces the specific interactions. The key residues involved for GN8 were ARG A:136 and ASN A:159, and HIS A:187, only PubChem CID 121982904 and CID 80305718, which show similar interactions with amino acid ASN A:159.

## 5 Conclusion

The novel identified potential anti-prion compounds through comparative molecular docking, pharmacophore modelling, and

TABLE 7 List of potential stabilizing compounds of Anle138b derived against Prion Protein (PDB 1QLZ) with their amino acid involved and binding affinity.

PubChem CID	Ligand	Amino acids	Interactions	Binding affinity (kcal/mol)
81158051	1-[2-(3-Fluorophenoxy)propanoylamino]cyclobutane-1-carboxylic acid (AKOS019729062)	GLU A:152 ASP A:202, ASN A:153, ARG A:156 PHE A:198 TYR A:149 TYR A:157, ASN A:197, THR A:199, GLU A:196	Halogen (Fluorine) Conventional hydrogen bond Pi-alkyl, alkyl Carbon-hydrogen bond Van-der waals	-5.9
81626642	4-(4,4-Dimethylazepane-1-carbonyl)-3,5-dimethyl-1H-pyrrole-2-carboxylic acid (AKOS020206072)	GLU A:196, HIS A:155 ARG A:156 HIS A:187 ARG A:136, TYR A:157, ASN A:159, PRO A:158, GLN A:160, TYR A:162, LEU A:130, THR A:191	Conventional hydrogen bond, Unfavourable acceptor-acceptor, Pi-alkyl, Van-der waals	-5.8
121982904	1-[2-(3-Methylphenoxy)butanoylamino]cyclobutane-1-carboxylic acid (AKOS027094107)	TYR A:157, ASN A:159 HIS A:187 TYR A:162 PRO A:158 THR A:191, THR A:190, GLN A:186, THR A:183, GLN A:160, LEU A:130, ARG A:156	Conventional hydrogen bond, Pi-Pi T-shaped, Pi-alkyl, Carbon-hydrogen bond, Van-der waals	-5.8
80305718	2-[2-(4-Fluoro-2-methylphenyl)ethylcarbamoylamino]-2-methylbutanoic acid (AKOS018868382)	GLN A:186 ASN A:159, TYR A:157 TYR A:162 HIS A:187, PRO A:158 THR A:190, THR A:183, ARG A:136, HIS A:155, ARG A:156, GLN A:160, LEU A:130	Halogen (Fluorine), Conventional hydrogen bond, Pi-Pi T-shaped, Carbon-hydrogen bond, pi-donor, hydrogen bond, Van-der waals	-6.0

ADMET analysis, showing a similar binding interaction at the residual level, suggesting them as potential candidates for a therapeutic approach. This includes molecular docking with known inhibitors (anle138b, resveratrol, and GN8) to highlight critical interactions involving both prion proteins (PDB ID: 1QLZ) and amyloid fibrils (PDB ID: 6LNI). Of these, anle138b and resveratrol showed strong binding to the fibril, while GN8 displayed favourable interactions with the prion protein, which was in agreement with their proposed mechanisms. Among the derived compounds, PubChem CIDs 133480707, 69849109, and 121982904 exhibited significant binding affinities, passed the ADMET selection criteria, and showed blood-brain barrier permeability, suggesting their suitability for further preclinical investigation. By targeting the autocatalytic secondary nucleation nature of PrP<sup>sc</sup>, through which aggregates proliferate, these molecules may potentially interfere with further growth and accumulation of prion protein and can effectively suppress prion propagation and aggregation. However, additional validation through molecular dynamics simulations, interaction fingerprinting, or *in vitro/in vivo* assays is critical to validate their efficacy. In addition, a comprehensive study that integrates experimental validation along with simulation could pave the way towards effective treatments for prions and other aggregation-associated neurodegenerative disorders.

## Data availability statement

The raw data supporting the conclusions of this article will be made available by the authors, without undue reservation.

## Author contributions

KR: Writing – original draft, Formal Analysis, Data curation, Investigation, Methodology, Writing – review and editing. SU: Writing – review and editing, Methodology, Writing – original draft. SM: Writing – review and editing. HD-A: Writing – review and editing. SC: Funding acquisition, Software, Writing – review and editing, Writing – original draft, Supervision, Investigation, Formal Analysis, Project administration, Data curation, Methodology, Validation, Conceptualization.

## Funding

The authors declare that financial support was received for the research and/or publication of this article. This work was supported by an Extramural Indian Council of Medical Research Grant (ICMR), India (EMDR/SG/11/2023-2353) and Institute of Eminence, Faculty Recharge Programme Grant, University of Delhi (ref. No./IOE/2023-24/12/FRP; Ref. No./IoE/2025-26/12/FRP) funded to Sumit K Chaturvedi. This work has been partially funded by the University Grants Commission (UGC) JRF (231610137930), India, awarded to Kamakshi Ruhela.

## Conflict of interest

The authors declare that the research was conducted in the absence of any commercial or financial relationships that could be construed as a potential conflict of interest.

The author(s) declared that they were an editorial board member of Frontiers, at the time of submission. This had no impact on the peer review process and the final decision.

## Generative AI statement

The authors declare that no Generative AI was used in the creation of this manuscript.

Any alternative text (alt text) provided alongside figures in this article has been generated by Frontiers with the support of artificial intelligence and reasonable efforts have been made to ensure

accuracy, including review by the authors wherever possible. If you identify any issues, please contact us.

## Publisher's note

All claims expressed in this article are solely those of the authors and do not necessarily represent those of their affiliated organizations, or those of the publisher, the editors and the reviewers. Any product that may be evaluated in this article, or claim that may be made by its manufacturer, is not guaranteed or endorsed by the publisher.

## References

- Alvarez-Martinez, M. T., Fontes, P., Zomosa-Signoret, V., Arnaud, J. D., Hingant, M., Pujo-Menjouet, D. M., et al. (2011). Dynamics of polymerization shed light on the mechanisms that lead to multiple amyloid structures of the prion protein. *Biochim Biophys Acta* 1814 (10): 1305–17. doi:10.1016/j.bbapap.2011.05.016
- Asher, D. M., and Gregori, L. (2018). Human transmissible spongiform encephalopathies: historic view. *Handb. Clin. Neurol.* 153, 1–17. doi:10.1016/b978-0-444-63945-5.00001-5
- Bagyinszky, E., Giau, V. V., Youn, Y. C., A An, S. S., and Kim, S. (2018). Characterization of mutations in PRNP (prion) gene and their possible roles in neurodegenerative diseases. *Neuropsychiatric Dis. Treat.* 14, 2067–2085. doi:10.2147/ndt.S165445
- Barreca, M. L., Iraci, N., Biggi, S., Cecchetti, V., and Biasini, E. (2018). Pharmacological agents targeting the cellular prion protein. *Pathogens* 7 (1), 27. doi:10.3390/pathogens7010027
- Béringue, V., Vilotte, J. L., and Laude, H. (2008). Prion agent diversity and species barrier. *Vet. Res.* 39 (4), 47. doi:10.1051/vetres:2008024
- Bernardi, L., and Bruni, A. C. (2019). Mutations in prion protein gene: pathogenic mechanisms in C-Terminal vs. N-Terminal domain, a review. *Int. J. Mol. Sci.* 20 (14), 3606. doi:10.3390/ijms20143606
- Collinge, J. (2001). Prion diseases of humans and animals: their causes and molecular basis. *Annu. Rev. Neurosci.* 24, 519–550. doi:10.1146/annurev.neuro.24.1.519
- Copyright © (2002). *National academy of sciences.*
- Cunha, J. E. G., Nascimento, J. C. F., and Oliveira, J. R. M. (2021). CJD without borders. *Nat. Rev. Neurol.* 17 (11), 723. doi:10.1038/s41582-021-00566-w
- Doh-Ura, K., Iwaki, T., and Caughey, B. (2000). Lysosomotropic agents and cysteine protease inhibitors inhibit scrapie-associated prion protein accumulation. *J. Virol.* 74 (10), 4894–4897. doi:10.1128/jvi.74.10.4894-4897.2000
- Doh-ura, K., Ishikawa, K., Murakami-Kubo, I., Sasaki, K., Mohri, S., Race, R., et al. (2004). Treatment of transmissible spongiform encephalopathy by intraventricular drug infusion in animal models. *J. Virol.* 78 (10), 4999–5006. doi:10.1128/jvi.78.10.4999-5006.2004
- Elmessaoudi-Idrissi, M., Blondel, A., Kettani, A., Windisch, M. P., Benjelloun, S., and Ezzikouri, S. (2018). Virtual screening in hepatitis B virus drug discovery: current State-of-the-art and future perspectives. *Curr. Med. Chem.* 25 (23), 2709–2721. doi:10.2174/0929867325666180221141451
- Geschwind, M. D. (2010). Rapidly progressive dementia: prion diseases and other rapid dementias. *Contin. (Minneapolis)* 16 (2 Dementia), 31–56. doi:10.1212/01.CON.0000368211.79211.4c
- Geschwind, M. D. (2015). Prion diseases. *Contin. (Minneapolis)* 21 (6 Neuroinfectious Disease), 1612–1638. doi:10.1212/con.00000000000000251
- Giordano, D., Biancanello, C., Argenio, M. A., and Facchiano, A. (2022). Drug design by pharmacophore and virtual screening approach. *Pharm. (Basel)* 15 (5), 646. doi:10.3390/ph15050646
- Guan, L., Yang, H., Cai, Y., Sun, L., Di, P., Li, W., et al. (2019). ADMET-score - a comprehensive scoring function for evaluation of chemical drug-likeness. *Medchemcomm* 10 (1), 148–157. doi:10.1039/c8md00472b
- Huang, W. J., Chen, W. W., and Zhang, X. (2015). Prions mediated neurodegenerative disorders. *Eur. Rev. Med. Pharmacol. Sci.* 19 (21), 4028–4034.
- Imran, M., and Mahmood, S. (2011). An overview of human prion diseases. *Virology* 438, 559. doi:10.1186/1743-422x-8-559
- Institute of Medicine Forum on Emerging, Infections (2002). “The national academies collection: reports funded by national institutes of health,” in *The emergence of zoonotic diseases: understanding the impact on animal and human health: workshop summary*. Editors Burroughs, T., Knobler, S., and Lederberg, J. (Washington (DC): National Academies Press US).
- Jankovska, N., Rusina, R., Bruzova, M., Parobkova, E., Olejar, T., and Matej, R. (2021). Human prion disorders: review of the current literature and a twenty-year experience of the national surveillance center in the Czech Republic. *Diagn. (Basel)* 11 (10), 1821. doi:10.3390/diagnostics11101821
- Jarrett, J. T., and Lansbury, P. T., Jr. (1993). Seeding “one-dimensional crystallization” of amyloid: a pathogenic mechanism in Alzheimer’s disease and scrapie? *Cell* 73 (6), 1055–1058. doi:10.1016/0092-8674(93)90635-4
- Jeong, J. K., Moon, M. H., Bae, B. C., Lee, Y. J., Seol, J. W., Kang, H. S., et al. (2012). Autophagy induced by resveratrol prevents human prion protein-mediated neurotoxicity. *Neurosci. Res.* 73 (2), 99–105. doi:10.1016/j.neures.2012.03.005
- Kimura, T., Sako, T., Kuwata, K., Hosokawa-Muto, J., Hosokawa-Muto, J., Cui, Y. L., et al. (2013). Synthesis of an (11) C-labeled antiprion GN8 derivative and evaluation of its brain uptake by positron emission tomography. *ChemMedChem* 8 (7), 1035–1039. doi:10.1002/cmdc.201300167
- Kuwata, K., Li, H., Yamada, H., Legname, G., Prusiner, S. B., Akasaka, K., et al. (2002). Locally disordered conformer of the hamster prion protein: a crucial intermediate to PrP<sup>Sc</sup>? *Biochemistry* 41 (41), 12277–12283. doi:10.1021/bi026129y
- Kuwata, K., Nishida, N., Matsumoto, T., Kamatari, Y. O., Hosokawa-Muto, J., Kodama, K., et al. (2007). Hot spots in prion protein for pathogenic conversion. *Proc. Natl. Acad. Sci. U S A* 104 (29), 11921–11926. doi:10.1073/pnas.0702671104
- Leidel, F., Eiden, M., Geissen, M., Kretzschmar, H. A., Giese, A., Hirschberger, T., et al. (2011). Diphenylpyrazole-derived compounds increase survival time of mice after prion infection. *Antimicrob. Agents Chemother.* 55 (10), 4774–4781. doi:10.1128/aac.00151-11
- Li, L., Zhu, Y., Zhou, S., An, X., Zhang, Y., Bai, Q., et al. (2017). Experimental and theoretical insights into the inhibition mechanism of prion fibrillation by resveratrol and its derivatives. *ACS Chem. Neurosci.* 8 (12), 2698–2707. doi:10.1021/acschemneuro.7b00240
- Maiti, N. R., and Surewicz, W. K. (2001). The role of disulfide bridge in the folding and stability of the recombinant human prion protein. *J. Biol. Chem.* 276 (4), 2427–2431. doi:10.1074/jbc.M007862200
- Manix, M., Kalakoti, P., Henry, M., Thakur, J., Menger, R., Guthikonda, B., et al. (2015). Creutzfeldt-jakob disease: updated diagnostic criteria, treatment algorithm, and the utility of brain biopsy. *Neurosurg. Focus* 39 (5), E2. doi:10.3171/2015.8.Focus15328
- Matthes, D., Gapsys, V., Griesinger, C., and de Groot, B. L. (2017). Resolving the atomistic modes of Anle138b inhibitory action on peptide oligomer formation. *ACS Chem. Neurosci.* 8 (12), 2791–2808. doi:10.1021/acschemneuro.7b00325
- McKinley, M. P., Bolton, D. C., and Prusiner, S. B. (1983). A protease-resistant protein is a structural component of the scrapie prion. *Cell* 35 (1), 57–62. doi:10.1016/0092-8674(83)90207-6
- Meng, X. Y., Zhang, H. X., Mezei, M., and Cui, M. (2011). Molecular docking: a powerful approach for structure-based drug discovery. *Curr. Comput. Aided-Drug Des.* 7 (2), 146–157. doi:10.2174/157340911795677602
- Nafe, R., Arendt, C. T., and Hattingen, E. (2023). Human prion diseases and the prion protein - what is the current state of knowledge? *Transl. Neurosci.* 14 (1), 20220315. doi:10.1515/tnsci-2022-0315
- Pan, K. M., Baldwin, M., Nguyen, J., Gasset, M., Serban, A., Groth, D., et al. (1993). Conversion of alpha-helices into beta-sheets features in the formation of the scrapie prion proteins. *Proc. Natl. Acad. Sci. U S A* 90 (23), 10962–10966. doi:10.1073/pnas.90.23.10962

- Paterson, R. W., Takada, L. T., and Geschwind, M. D. (2012). Diagnosis and treatment of rapidly progressive dementias. *Neurol. Clin. Pract.* 2 (3), 187–200. doi:10.1212/CPJ.0b013e31826b2ae8
- Peters, P. J., Mironov, A., Jr., Peretz, D., van Donselaar, E., Leclerc, E., Erpel, S., et al. (2003). Trafficking of prion proteins through a caveolae-mediated endosomal pathway. *J. Cell Biol.* 162 (4), 703–717. doi:10.1083/jcb.200304140
- Petit, C. S., Besnier, L., Morel, E., Rousset, M., and Thenet, S. (2013). Roles of the cellular prion protein in the regulation of cell-cell junctions and barrier function. *Tissue Barriers* 1 (2), e24377. doi:10.4161/tisb.24377
- Plascencia-Villa, G., and Perry, G. (2023). Roles of oxidative stress in synaptic dysfunction and neuronal cell death in alzheimer's disease. *Antioxidants (Basel)* 12 (8), 1628. doi:10.3390/antiox12081628
- Prusiner, S. B. (1982). Novel proteinaceous infectious particles cause scrapie. *Science* 216 (4542), 136–144. doi:10.1126/science.6801762
- Prusiner, S. B. (1998). Prions. *Proc. Natl. Acad. Sci. U S A* 95 (23), 13363–13383. doi:10.1073/pnas.95.23.13363
- Prusiner, S. B. (2001). Neurodegenerative diseases and prions. *N. Engl. J. Med.* 344 (20), 1516–1526. doi:10.1056/nejm200105173442006
- Qin, P., Sun, Y., and Li, L. (2024). Mitochondrial dysfunction in chronic neuroinflammatory diseases (review). *Int. J. Mol. Med.* 53 (5), 47. doi:10.3892/ijmm.2024.5371
- Riesner, D. (2003). Biochemistry and structure of PrP(C) and PrP(Sc). *Br. Med. Bull.* 66, 21–33. doi:10.1093/bmb/66.1.21
- Rizvi, S. M., Shakil, S., and Haneef, M. (2013). A simple click by click protocol to perform docking: autodock 4.2 made easy for non-bioinformaticians. *Excli J.* 12, 831–857.
- Roucou, X., Gains, M., and LeBlanc, A. C. (2004). Neuroprotective functions of prion protein. *J. Neurosci. Res.* 75 (2), 153–161. doi:10.1002/jnr.10864
- Sejvar, J. J., Schonberger, L. B., and Belay, E. D. (2008). Transmissible spongiform encephalopathies. *J. Am. Veterinary Med. Assoc.* 233 (11), 1705–1712. doi:10.2460/javma.233.11.1705
- Sigurdson, C. J., and Miller, M. W. (2003). Other animal prion diseases. *Br. Med. Bull.* 66 (1), 199–212. doi:10.1093/bmb/66.1.199
- Sunseri, J., and Koes, D. R. (2016). Pharmit: interactive exploration of chemical space. *Nucleic Acids Res.* 44 (W1), W442–W448. doi:10.1093/nar/gkw287
- Surewicz, W. K., and Apostol, M. I. (2011). Prion protein and its conformational conversion: a structural perspective. *Top. Curr. Chem.* 305, 135–167. doi:10.1007/128\_2011\_165
- Tee, B. L., Longoria Ibarrola, E. M., and Geschwind, M. D. (2018). Prion diseases. *Neurol. Clin.* 36 (4), 865–897. doi:10.1016/j.ncl.2018.07.005
- Thompson, M. J., Louth, J. C., Little, S. M., Chen, B., and Coldham, I. (2011). 2,4-diarylthiazole antiprion compounds as a novel structural class of antimalarial leads. *Bioorg. and Med. Chem. Lett.* 21 (12), 3644–3647. doi:10.1016/j.bmcl.2011.04.090
- Trevitt, C. R., and Collinge, J. (2006). A systematic review of prion therapeutics in experimental models. *Brain* 129 (Pt 9), 2241–2265. doi:10.1093/brain/aw1150
- Tsuboi, Y., Doh-ura, K., and Yamada, T. (2009). Continuous intraventricular infusion of pentosan polysulfate: clinical trial against prion diseases. *Neuropathology* 29 (5), 632–636. doi:10.1111/j.1440-1789.2009.01058.x
- Ugbaja, S. C., Mushebenge, A. G. A., Kumalo, H., Ngcobo, M., and Gqaleni, N. (2025). Potential benefits of *in silico* methods: a promising alternative in natural compound's drug discovery and repurposing for HBV therapy. *Pharmaceuticals* 18 (3), 419. doi:10.3390/ph18030419
- Uliassi, E., Nikolic, L., Bolognesi, M. L., and Legname, G. (2023). Therapeutic strategies for identifying small molecules against prion diseases. *Cell Tissue Res.* 392 (1), 337–347. doi:10.1007/s00441-021-03573-x
- Uttley, L., Carroll, C., Wong, R., Hilton, D. A., and Stevenson, M. (2020). Creutzfeldt-Jakob disease: a systematic review of global incidence, prevalence, infectivity, and incubation. *Lancet Infect. Dis.* 20 (1), e2–e10. doi:10.1016/s1473-3099(19)30615-2
- Vallabh, S. M., Zou, D., Pitsstick, R., O'Moore, J., Peters, J., Silvius, D., et al. (2023). Therapeutic trial of anle138b in mouse models of genetic prion disease. *J. Virol.* 97 (2), e01672-22. doi:10.1128/jvi.01672-22
- Vey, M., Pilkuhn, S., Wille, H., Nixon, R., DeArmond, S. J., Smart, E. J., et al. (1996). Subcellular colocalization of the cellular and scrapie prion proteins in caveolae-like membranous domains. *Proc. Natl. Acad. Sci. U S A* 93 (25), 14945–14949. doi:10.1073/pnas.93.25.14945
- Viles, J. H., Donne, D., Kroon, G., Prusiner, S. B., Cohen, F. E., Dyson, H. J., et al. (2001). Local structural plasticity of the prion protein. Analysis of NMR relaxation dynamics. *Biochemistry* 40 (9), 2743–2753. doi:10.1021/bi002898a
- Wagner, J., Ryazanov, S., Leonov, A., Levin, J., Shi, S., Schmidt, F., et al. (2013). Anle138b: a novel oligomer modulator for disease-modifying therapy of neurodegenerative diseases such as prion and Parkinson's disease. *Acta Neuropathol.* 125 (6), 795–813. doi:10.1007/s00401-013-1114-9
- Wan, W., Wille, H., Stöhr, J., Kendall, A., Bian, W., McDonald, M., et al. (2015). Structural studies of truncated forms of the prion protein PrP. *Biophys. J.* 108 (6), 1548–1554. doi:10.1016/j.bpj.2015.01.008
- Wermuth, C. G. (2004a). Multitargeted drugs: the end of the "one-target-one-disease" philosophy? *Drug Discov. Today* 9 (19), 826–827. doi:10.1016/s1359-6446(04)03213-1
- Wermuth, C. G. (2004b). Selective optimization of side activities: another way for drug discovery. *J. Med. Chem.* 47 (6), 1303–1314. doi:10.1021/jm030480f
- Wille, H., and Requena, J. R. (2018). The structure of PrP(Sc) prions. *Pathogens* 7 (1), 20. doi:10.3390/pathogens7010020
- Wulf, M. A., Senatore, A., and Aguzzi, A. (2017). The biological function of the cellular prion protein: an update. *BMC Biol.* 15 (1), 34. doi:10.1186/s12915-017-0375-5
- Yamasaki, T., Suzuki, A., Hasebe, R., and Horiuchi, M. (2014). Comparison of the anti-prion mechanism of four different anti-prion compounds, anti-PrP monoclonal antibody 44B1, pentosan polysulfate, chlorpromazine, and U18666A, in prion-infected mouse neuroblastoma cells. *PLoS One* 9 (9), e106516. doi:10.1371/journal.pone.0106516
- Zahn, R., Liu, A., Lührs, T., Riek, R., von Schroetter, C., López García, F., et al. (2000). NMR solution structure of the human prion protein. *Proc. Natl. Acad. Sci. U S A* 97 (1), 145–150. doi:10.1073/pnas.97.1.145